

Feasibility of low q-space diffusion MRI at 1.5T

Henry H. Ong¹, Yusuf Bhagat¹, Jeremy Magland¹, and Felix W. Wehrli¹

¹Laboratory for Structural NMR Imaging, Department of Radiology, University of Pennsylvania School of Medicine, Philadelphia, PA, United States

Introduction

By exploiting the regularity of molecular diffusion restrictions such as axon membranes and myelin sheaths¹, q-space imaging^{2,3} (QSI) offers potential for indirect assessment of white matter (WM) axonal architecture. For example, QSI can accurately estimate mean axon diameter (MAD) and intracellular volume fraction (ICF)^{4,5}. Unfortunately, the application of QSI on a clinical scanner is severely constrained by the low gradient strengths available, which limits the maximum achievable q-value ($q = (2\pi)^{-1}\gamma G\delta$, G = gradient amplitude, and δ = gradient duration). Low maximum q-value leads to insufficient displacement resolution to accurately study axons, which have an MAD of 1-3 μm . Low q-value diffusion MRI⁵, in which axonal architecture information is extracted by fitting the q-space signal decay ($E(q)$) at low q-values ($q^{-1} \gg \text{MAD}$) under the short gradient pulse approximation (SGPA), does not require high gradient amplitudes. However, low clinical gradient strengths lead to violation of SGPA. Here, we test the feasibility of implementing low q-value diffusion MRI on a 1.5T system by assessing axonal architecture in excised fixed pig spinal cords.

Methods

As described in [5], at low q-values ($q^{-1} \gg \text{MAD}$), the signal decay is given by $E(q) = \exp(-2\pi^2 q^2 Z^2)$ (Eq. 1), where Z is the root mean squared (RMS) displacement of diffusing molecules during a diffusion time Δ ^{6,7}. As $E(q)$ contains signal from extra- and intra-cellular spaces (ECS and ICS), a two-compartment version of Eq. 1 can be defined: $E(q) = f_E \exp(-2\pi^2 q^2 Z_E^2) + f_I \exp(-2\pi^2 q^2 Z_I^2)$ (Eq. 2), where f_E and f_I are the relaxation-weighted ECS and ICS volume fractions and Z_E and Z_I are the RMS displacement of diffusing molecules in the ECS and ICS. From Eq. 2, MAD and ICF can be estimated from Z_I and f_I , respectively.

For validation of this method, five fixed cervical spinal cords (SC) harvested from five skeletally mature Yucatan mini-pigs were used. Before experiments, the SCs were placed in tubes filled with Fomblin (Sigma-Aldrich) to keep the specimens hydrated and to remove any background signal. The low q-value diffusion MRI method was implemented on a 1.5T Siemens Sonata MRI scanner (Erlangen, Germany) with 40 mT/m gradients using a custom single-slice PGSE with multi-shot fly-back EPI readout pulse sequence. The body coil was used for transmit and a custom-built 4-channel phased array coil (Insight MRI) was used for receive. The imaging parameters were: $\Delta/\delta/TE = 98.7/55/257\text{ms}$, 128×128 , $FOV = 64 \times 64$ mm, slice thickness = 10 mm, number of shots = 8, $NA = 36$, and $TR = 2$ s. The diffusion gradient was applied perpendicular to the SCs in 32 increments ($q_{\text{max}} = 0.08 \mu\text{m}^{-1}$) and the scan time ~ 5 hours. Note that these values for δ and Δ violate SGPA. All five SCs were imaged simultaneously. After Fourier transform, a 3D matrix of 32 2D images at various q-values was obtained. An average $E(q)$ was measured in ROIs within the dorsal, ventral, and lateral columns of the SCs (Fig. 1). This average $E(q)$ was fit with Eq. 2 under the constraint $f_E + f_I = 1$.

Results and Discussion

Fig. 2 shows a sample $E(q)$ with the fit from Eq. 2. The fit shows good agreement with $E(q)$ ($R^2 > 0.98$). For display purposes, a one-compartment fit (Eq. 1) is also shown to illustrate its poor agreement. Fig. 3 shows bar graphs of f_E , Z_E , f_I , and Z_I fitting results for each ROI averaged over all five SCs. Z_I falls

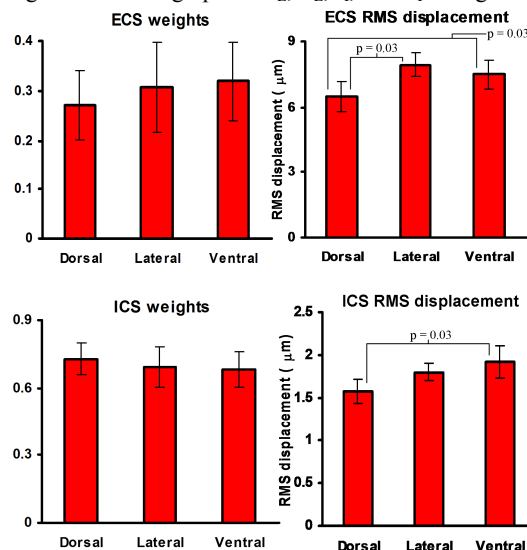


Fig. 3. Bar graphs of f_E (ECS weighting), Z_E (ECS RMS displacement), f_I (ICS weighting), and Z_I (ICS RMS displacement) fitting results. Standard deviation bars are shown. Significant p-values (< 0.05) of paired t-tests between the different ROIs are shown.

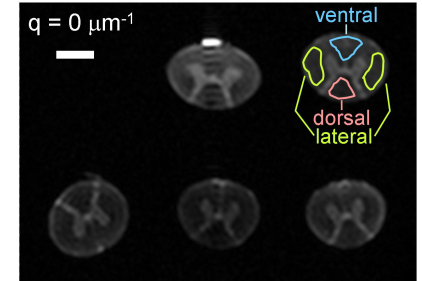


Fig. 1. Sample image at $q = 0 \mu\text{m}^{-1}$. White bar = 5 mm. ROI locations are shown for the dorsal, ventral and lateral WM columns. The bright spot above the center top SC is residual surface PBS.

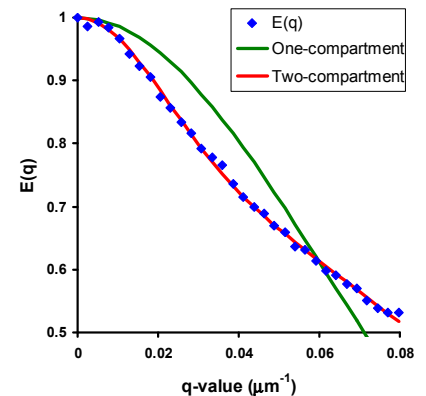


Fig. 2. Sample $E(q)$ for a lateral WM column ROI (blue diamonds) with one-compartment (green line) and two-compartment (red line) fits.

within 1-2 μm , which is the expected range of axon diameters in mammals⁸. Z_E is lower than that expected for free water ($\sim 20\mu\text{m}$ for $\Delta = 98.7\text{ms}$). The ADC calculated from Z_E ($\sim 0.25 \times 10^{-3} \text{mm}^2/\text{s}$) agrees with literature values for fixed spinal cord WM tissue⁹, which provides further evidence that ADCs measured at low b-values ($< 2500 \text{s/mm}^2$) primarily reflect diffusion in ECS¹⁰. The average f_I was ~ 0.7 , which falls within the expected ICF for WM¹¹. An ANOVA analysis indicated no significant differences in f_I among the WM columns as previously seen in mouse SP⁵. Paired t-tests indicated that the dorsal column Z_E and Z_I are significantly smaller than those of the ventral WM column, which matches previous observations of smaller MAD and increased axon density in the dorsal compared with ventral columns^{4,8,9}.

Conclusion

This work demonstrates the feasibility of implementing low q-value diffusion MRI on a 1.5T scanner. The results show that despite violating SGPA, this method has the potential to accurately assess regional axonal architecture with metrics such as MAD and ICF.

References: 1. Beaulieu, C, *NMR Biomed*, **15**:435 (2002). 2. Callaghan, PT, *Principles of NMR Microscopy*, Oxford University Press (1991). 3. Cohen, Y, *et al.*, *NMR Biomed*, **15**:516 (2002). 4. Ong, HH, *Neuroimage*, **40**:1619 (2008). 5. Ong, HH, *Neuroimage*, **51**:1360 (2010). 6. Price W, *Concepts Magn Res*, **10**:299 (1997). 7. Kimmich R, *NMR: Tomography, Diffusometry, Relaxometry*, Springer-Verlag (1997). 8. Williams, PL, *et al.*, *Gray's anatomy*, Churchill Livingstone (1995). 9. Schwartz, ED, *et al.*, *AJNR*, **26**:390 (2005). 10. Schwartz, E.D., *et al.*, *Neuroreport*, **16**:73 (2005). 11. Sykova, E, *et al.*, *Physiol Rev*, **88**:1277 (2008). **Acknowledgements:** NIH R21 EB003951